Analysis of externally loaded bolted joints: Analytical, computational and experimental study

J. G. Williams, R. E. Anley, D. H. Nash, T. G. F. Gray*

Department of Mechanical Engineering, University of Strathclyde, G1 1XJ, UK

Abstract

The behaviour of a simple single-bolted-joint under tensile separating loads is analysed using conventional analytical methods, a finite element approach and experimental techniques. The variation in bolt force with external load predicted by the finite element analysis conforms well to the experimental results. It is demonstrated that certain detailed features such thread interaction do not need to be modelled to ensure useful results. Behaviour during the pre-loading phase of use agrees with previous long-standing studies. However, the pre-loading analysis does not carry over to the stage when external loading is applied, as is normally assumed and it is shown that the current, conventional analytical methods substantially over-predict the proportion of the external load carried by the bolt. The basic reason for this is shown to be related to the non-linear variation in contact conditions between the clamped members during the external loading stage.

Keywords: bolted joints, pre-loading, bolt stiffness, member stiffness, member contact

Nomenclature

Symbol	Definition	SI Unit
C	Fraction of external load carried by bolt (or 'joint stiffness parameter' as defined by Eqn (3))	-
d	Bore diameter	m
D	Diameter of washer (or bolt head) in contact with clamped member	m
A_s	Bolt shank area	m^2
E	Young's Modulus	N/m^2
F_b	Resultant bolt load	N
F_i	Pre-load in the bolt	N
F_m	Resultant member load	N
k_b	Bolt stiffness	N/m
k_m	Total member stiffness	N/m
L	Grip length (= t_{m1}+t_{m2})	m
P	External separating load	N
P_b	Load in bolt (or additional load carried by bolt in external loading stage)	N

* Corresponding author: Tel. +44 141 776 3569; Fax = 44 141 552 5105
E-mail address: tom.gray@virgin.net

P_m	External load taken by members	N
t_{m1}	Thickness of member 1 (upper)	m
t_{m2}	Thickness of member 2 (lower)	m
α	Half apex angle of pressure cone (taken as 30° in this study)	deg
β	Ratio of bolt/nut outside diameter to bolt diameter	
μ_k	Coefficient of dynamic friction	-
μ_s	Coefficient of static friction	-
υ	Poisson's Ratio	-

1.0 Introduction

The investigation described herein was prompted in the first instance by anomalies revealed during design analysis of high-integrity, metal-to-metal, pressurised flanges. An important criterion in the design of such joints is that the proportion of external service loading carried by the bolts should be as low as possible, in order to minimise the incidence of bolt fatigue failure. Critical service conditions were to be applied in the design case which gave rise to the study and finite element analyses were used to cross-check the standard or 'classical' design approach, as exemplified by references [1-5]. The unexpected outcome was that a large discrepancy in predicted bolt load was revealed between those classical methods which would be acceptable to approval authorities, and the special finite element analyses. This finding prompted a three-stage, systematic investigation, comprising analytical, experimental and computational studies of a representative bolt assembly (see Figure 1), exploration of contact modelling and non-linear effects in finite element analysis of such joints and, finally, a parametric analysis of an assembly to discover the main geometric influences on behaviour.

The present paper covers the first stage of the investigation, comparing the results of a finite element analysis with an experimental study. Several finite element studies are evident in the literature and these show that the contact conditions within a bolted joint are complex and introduce many uncertainties. However, there seem to be few examples in the literature where computational analyses have been validated directly by experiment.

2.0 Background

Bolted joints are often regarded as unreliable and a frequent source of failure in service. In situations where leakage would be regarded as catastrophic, all-welded pipework is often specified, despite the penalty this brings when disassembly is required. There are many reasons for this, including variability associated with sealing materials and lack of specification or skill in on-site assembly, but analytical uncertainties are also a significant factor.

Two main approaches to the design of pressure-containing, bolted flange joints can be recognised. In the first case, contact between the flanges is made through a flexible

seal or gasket and the bolts are sized and tightened initially to apply and maintain the correct gasket interface pressure. In the second case, the flanges are pulled together to make direct, face-to-face contact. If a seal is included in this case, it is set in a groove or chamber where the contact pressure conditions are determined by the geometry of the groove. Bolted joints may also of course have a purely load transmitting function and fluid sealing may not be a specific requirement.

The first type of gasket-contacting joint is covered in design terms by long-established standards, for example [6], notwithstanding the fact that it has distinct disadvantages from the strength point of view. The main strength problem lies in the fact that the compressive stiffness of the gasket is usually low relative to the tensile stiffness of the bolting and this means that the bolts will suffer a large fraction of any service or external load fluctuation, to the consequent detriment of fatigue life. Also, the typical configuration of gasket seals is such that large radial offsets usually exist between the pressure load, the gasket contact load and the bolt reactions and this gives rise to large radial bending moments in the flanges and possibly also bending of the bolts.

In the second form of joint, where the flanges contact directly, the clamped members are relatively stiff in compression and therefore the in-service fluctuations of bolt load are likely to be small or negligible, provided that the bolts are tightened initially to a level exceeding the expected external load and also that the flanges do not separate. If the seal has a small radial dimension, or a face-to-face sealing strategy is adopted, the overall diameter of the flanges can be reduced relative to the pipe dimensions, with consequent reductions in flange and bolt bending effects. These principles have been worked out in various forms of special flange, with the generic title of 'compact' flange [7]. However, such designs have not been widely accepted, despite the significant gains in weight-saving and performance that they can bring. Reluctance to change from a formally accepted Standard may be one reason for this, but the nature of the analytical uncertainties which prompted the present study may be another. It is therefore of interest to remove such uncertainties to allow the full potential of the compact flange design to be realised.

3. Theory

The conventional or classical theory of bolted joints is widely accepted and enshrined in many engineering textbooks e.g. [1-5]. Conventional theory is based on the premise that the bolt and the sandwiched members of a given bolted joint configuration can each be modelled as linear springs having stiffness k_b and k_m respectively, acting in parallel.

From the basic definition of stiffness and the principles of equilibrium and compatibility, the following relations for the bolt force, F_b, and member force, F_m, shown in Figure 1, can be obtained:

$$F_b = CP + F_i = P_b + F_i \qquad \text{…Eqn (1)}$$

$$F_m = (1 - C)P - F_i = P_m - F_i \qquad \text{…Eqn (2)}$$

Where F_i is the bolt pre-load, P_b is the portion of the external load carried by the bolt, P_m is the portion of the external load taken by the members and C is the joint stiffness parameter defined as:

$$C = \frac{k_b}{k_b + k_m} \qquad \text{…Eqn (3)}$$

The above equations should hold, provided that member bending or rotational effects are negligible, and that sufficient initial compression remains to prevent the members from separating.

Bolt stiffness is normally obtained by considering the portion of the bolt contained in the joint as a uniform bar in tension:

$$k_b = \frac{A_s E_b}{L} \qquad \text{…Eqn (4)}$$

This formulation treats the bolt head and nut as regions as rigid and various authors (eg Bickford [4]) have suggested that the length L should be augmented by a proportion of the bolt diameter d to give an equivalent length L_{eq} which recognises the contribution of strains in the head/nut to extension of the bolt under load. A more recent formulation by N.L. Pedersen and P. Pedersen [8] based on finite element computation, also involves the outside diameter of the bolt/nut or washer, expressed as a ratio β relative to the bolt diameter, and the influence of Poisson's ratio in the head/nut regions. This relation is given as:

$$L_{eq} = L + (1.95 - \frac{\beta}{2} - \upsilon)d \qquad \text{…Eqn (5)}$$

Calculation of member stiffness is considerably more difficult due to the nature of the load diffusion from the bolt head and nut into the members. Motosh [9] and Burguete [10] review a large number of proposed methods for determining the stiffness of the clamped members. However, the most commonly used analytical procedure is the 'pressure-cone' method in which the stress distribution in the members is approximated to a truncated cone shape of half-apex angle α. Outside this pressure-cone region, the magnitude of the stress field is considered to be negligible. The pressure cone geometry is indicated by the dashed line in Figure 2. By considering the deflection of a small element of the cone dy and integrating the effective load carrying area of the members with respect to the vertical position y, a general expression for member stiffness is obtained as follows:

$$k_m = \frac{\pi E_0 d \tan\alpha}{\ln\left[\dfrac{(2t_0 \tan\alpha + D_0 - d)(D_0 + d)}{(2t_0 \tan\alpha + D_0 + d)(D_0 - d)}\right]} \qquad \text{…Eqn (6)}$$

The stiffness of each sandwiched member is found by using appropriate substitutions for t_0, D_0 and E_0.

For the case where the thickness of the upper member is less than the thickness of the lower member, as in Figure 2, the stiffness of the upper member, k_{m1}, the first portion of the lower member, k_{m21}, and the second portion of the lower member, k_{m22}, can be determined by applying substitution sets (1), (2) and (3) respectively.

$$E_0 = E_1 \qquad t_0 = t_{m1} \qquad D_0 = D \qquad \text{…Set (1)}$$

$$E_0 = E_2 \qquad t_0 = \frac{t_{m2} - t_{m1}}{2} \qquad D_0 = 2t_{m1}\tan\alpha + D \qquad \text{…Set (2)}$$

$$E_0 = E_2 \qquad t_0 = \frac{t_{m2} + t_{m1}}{2} \qquad D_0 = D \qquad \text{…Set (3)}$$

Subsequently, the total member stiffness, k_m, is obtained from the standard relation for springs in series:

$$\frac{1}{k_m} = \frac{1}{k_{m1}} + \frac{1}{k_{m21}} + \frac{1}{k_{m22}} \qquad \text{…Eqn (7)}$$

For the particular case where the members are of equal thickness, $k_{m1} = k_{m2}$, $k_m = ½ k_{m1}$.

The value of the cone angle α to be assumed in the above relations has been the subject of much investigation. For example, Osgood [11], Wileman et al [12] and Lehnhoff et al [13, 14] have all studied the load diffusion path at the pre-load stage, using the finite element approach and have demonstrated that the cone angle depends somewhat on the particular joint configuration. Thus, as no unique cone angle exists, different engineering texts often adopt different values for α. Most are in the region of 30° and therefore a pressure cone angle of 30° was employed here for comparison with the classical approach. Reference [13] also notes that the inner radius of the member d (i.e the radius of the clearance hole) should be used in the member stiffness formulation (equation 6) and not the bolt shank diameter. This point has also been emphasised more recently by N.L. Pedersen and P. Pedersen [15] in a new formulation of member stiffness at the pre-load stage.

Note that it is assumed in this form of analysis that the member stiffness is linear at all times and is the same during the external loading stage as for the pre-loading operation. Grosse and Mitchell [16] provided evidence from a finite element study of a single geometry that these conditions might not prevail and that, in the external loading stage, the effective member stiffness can be both much higher than in the pre-loading stage and also non-linear.

In the present work, a simple single-bolted-joint arrangement of the type depicted in Figure 1 was analysed when subject to an increasing external load, applied in a sense that would separate the joint. The model should reasonably represent the behaviour of an individual bolt in a group comprising a connection, although the behaviour would not necessarily be axisymmetric in such a case. The forces in the bolt shank, predicted alternatively by classical analytical techniques and the FE computation, were compared to the experimental determination. Effects of gaskets and washers were not considered.

4.0 Experimental analysis

Figure 3 shows a wire frame model of the test assembly. The test specimen was designed such that it could be considered to be axisymmetric, thereby reducing the complexity of the required FE model. Figure 4 shows a representation of the assembly and details the important dimensions.

Classical bolted joint theory does not consider flange bending effects and these were minimised in the experimental model by restricting the outside diameter and thus, the loading radius. The test rig was attached to a tensile test machine by two externally threaded connecting shafts, screwed to the inside diameter of each cylinder. The

outside diameter of the bolted assembly was set at seven times the bolt diameter to ensure that load diffusion from the bolt head should not interact with the applied load or the outer boundary of the flange (i.e. in excess of the largest pressure cone angle of 45˚ suggested in the literature). A reserve factor of three on yield strength was applied to the loaded annulus to avoid plastic deformation in this region.

Aircraft Standard AS 21523 bolts and nuts, featuring integral washer contact were used. Two strain gauges were aligned axially on the bolt shank. The strain gauges were arranged in a full-bridge to reject bending strains. A clearance of 1.5 mm between the bolt shank and the bore was required for the strain gauges. The bolt was centrally aligned in the members by using locating washers with an internal profile that matched the outside profile of the bolt head and nut, and an outside diameter that corresponded to the internal diameter of the cylindrical rig wall.

5.0 Finite Element Model

A two-dimensional, axisymmetric model of the experiment was developed using the finite element code ANSYS v 9.0 [17] (see Figure 5). Dimensions were as given in Figure 4. (The inset diagram 'simplified bolt geometry' will be discussed later.) This idealisation introduced only minor geometric approximations, such as a cylindrical bolt head and nut. Accurate comparison of the FE results with the experimental results was the principal objective and the thread profiles were included in the model. Plasticity effects were also considered by employing the Bi-linear Kinematic Hardening model included in the ANSYS software, with a post yield modulus set at 10% of Young's Modulus. The material properties of the bolt and test rig are detailed in Table 1 and the coefficients of friction adopted are given Table 2. This model, incorporating detailed thread profiles and plasticity characterisation, is designated 'advanced model' in the results presentations.

The model was meshed with the two-dimensional, 2^{nd} order, quadrilateral element PLANE82, which has axi-symmetric capability. Flexible-to-flexible contact surfaces were defined between all contacting geometries. Contact surface pairs were generated using the contact elements CONTA172 and TARGE169, which are three-node, one-dimensional elements and are compatible with the PLANE82 elements used. The surfaces meshed with the CONTA172 elements allow penetration of the corresponding surfaces meshed with TARGE169. Hence for flexible-to-flexible contact analysis, each surface was meshed with both contact and target elements.

The pre-load in the bolt was generated at the mid-plane of the bolt shank using the pretension element PRETS179, which is contained in the ANSYS v9.0 element library. These elements allow direct specification of the pre-load in the bolt. Essentially, the pretension elements operate by splitting the geometry on a particular plane and subsequently collapsing elements across this location until the required pre-load is generated.

Due to the nature of operation of the pretension elements, it was necessary to apply vertical constraint to the model at the innermost node of the member-member interface. Consequently, loads closely approaching the value required to give complete separation of the joint were not considered. The external loading was

applied in terms of nodal point forces at the inner face of the annular wall of the rig (see Figure 5).

Inclusion of such features as the bolt and nut thread profiles in the finite element model adds greatly to the modelling overhead. Furthermore the geometry of the bi-hex bolt head used was difficult to generate. A simpler model of the experimental rig was developed therefore, in which the threads were removed and plasticity effects were excluded. The bolt head and nut geometries were simplified to a rectangular transverse sectional form (of external radius 5.6 mm as in the actual bolt). The simplified bolt geometry is shown on the left hand side of Figure 5 (note: all other geometric features were unchanged) and this model is described as 'simple FEA model' in the results presentation later.

6.0 Experimental and FEA results

The experimentally measured force in the bolt was obtained from the product of the recorded strain, the Young's modulus of the bolt and the shank area. The bolt force computed by FEA was calculated from the bolt area, together with the stress at the bolt mid-plane, which was consistently uniaxial and uniform.

The load data for the analysis is provided in Table 3. The strain gauges on the bolt shank were used to set the pretension in the experiment. The experimental procedure was repeated four times for each pre-tension value and good repeatability was achieved in all cases. A new bolt was used when applying a different pre-load. The external loading was increased in the experiments to a level corresponding to 70-80% of the respective pre-load.

Figures 6 and 7 compare the experimental results at two levels of pre-load choice, with those obtained from the FE analysis. In this presentation, the total bolt load P_b and the external load P are normalised with respect to the pre-load F_i, starting from the pre-load level, and the marker points indicate individual FE results at increasing loads.

Several observations can be made from the FEA plots. Firstly, the transfer of external load to the bolt is small in all cases. There are differences between the 'simple' and 'advanced' FEA results and the reasons for these differences relate to the effective stiffnesses of the bolt and member components at different stages, as shown in Table 4. (Note that in some cases, the force/displacement relationship for the component is not linear and the stiffness quoted is an average. Such results are preceded by '≅' sign.)

The lower transfer of load to the bolt in the 'advanced' model is due largely to the much greater member stiffness of the advanced model in the external loading stage, especially where the higher pre-load of 16/17 kN is applied. The most striking aspect of the stiffness table however, is that the member stiffnesses are substantially higher in the external loading stage than in the pre-load stage. This is of particular importance as conventional theory assumes that the stiffnesses do not change in moving from the pre-load to application of the external load. Pre-load level has little effect on the results from the 'simple' model, presumably because the material is assumed to be linear elastic and there is no 'bedding in' of the threads. Higher pre-

load results in a higher effective member stiffness in the 'advanced' model and slightly decreased bolt stiffness; these two factors leading to a greater reduction in bolt load relative to the 'simple' model. (It is arguable that a plasticity assumption is inappropriate for many applications in any case, as cyclic loading will usually result in shakedown to elastic behaviour.)
The non-linearity of the advanced model results has a number of sources, but the strongest influence is from the non-linearity of the member stiffness which reduces throughout, and especially as the external load reaches a level corresponding to the pre-load level. This leads to increased transfer of load to the bolt at higher external load levels. (Further explanation of these findings will be given later in the context of the stress fields.)

The computed behaviour is reflected fairly well in the experimental results, given the departures from idealisation, which are likely to be present, both in the finite element analyses and in the experimental determinations. Increasing the pre-load level in the experimental case reduces the transfer of load to the bolt (relatively) but not to such a great extent as predicted by the Advanced model.

Discrepancies between the finite element and experimental results can be attributed to several factors, including the following:

- Very small changes in the magnitude of the experimental bolt strains will generate large changes in measured force.
- The surface finish of members under the bolt head could not be made perfectly smooth due to the manufacturing difficulties associated with machining a blind hole. This, as suggested by Ito et al [18] can affect load diffusion from the bolt head. Reference [8] also highlights the strong influence on member stiffness of providing different forms of clearance under the bolt head or washer.
- The plasticity model applied in the FE model of the experimental arrangement is idealised and improved agreement might be obtained if the true post-yield material characteristics were to be modelled. Results from the FE model suggest localised yielding will occur both at the threads and at the corner where the bolt head joins the shank.
- The contact analysis capabilities of the FEA software and the influence of user specified parameters for contact analysis may contribute to the discrepancies.

The results from the simplified model happen to be closer to the experimental results, although this is probably fortuitous. This model does not capture the non-linear trends of the experimental curve, which would seem to be due mainly to local effects and plasticity. However, as the simple model should lead to a more conservative prediction of bolt force and is more robust from the modelling point of view, it has much to recommend it for use in the design of bolted connections.

7.0 Comparison with classical theory

The discrepancies between the experimental results and the results obtained from the finite element models become far less significant if the bolt loads predicted using classical theory (equations 1-7) are overlaid on the plots, as shown in Figure 8. This figure indicates that classical analytical techniques substantially over-estimate the load carried by the bolt, suggesting that bolted joints designed using this approach

appear to be much over-designed in terms of the increase in bolt load to be expected in service. This represents a considerable shift in design thinking and it is therefore advisable to establish the reasons for the large change in effective member stiffness which appears to take place when external load is applied.

The basic reason is that the boundary loading distribution of the external loading and the resulting effects on the contact at the interface between the members is too far removed from that of the pre-load case to be considered as equivalent, in terms of St Venant's Principle, to a separating load applied in the region of the bolt head. This is readily appreciated through Figures 9 and 10 which show contours of stress in the axial direction under pre-load and external loading conditions. (Note in these figures that the stress contour magnitudes are the same in each figure and the levels have been set to show the areas that carry high proportions of load, by virtue of their large cross-sectional area.)

Under pre-loading conditions, as shown in Figure 9, inter-member contact is maintained at both load levels and the increase of stress is linear, as is confirmed by load/deformation plots. Given that the outer radii correspond to larger areas, the whole cross section is seen to be carrying the pre-load, despite the fact that the stress in the outer radii is less. The most highly stressed area is not conical, of course, but it would be possible to define a conical region which would yield similar member stiffness to the computed value. The member stiffnesses, given in Table 4, are consistent with other determinations, including the most recent formulation in reference [15] and the barrel-shaped contours seen here have been noted in several other studies.

When the external loading is applied, as shown in Figure 10, the members begin to lose contact and the axial stress in the outer diameter regions of the member drops to zero, or at least to a low level. The member rapidly sheds much of the load corresponding to the previous pre-load stress fields. Note that the stress field close to the bolt head contact changes very little. As a consequence, the effective unloading stiffness of the member is high and very little of the external load is transmitted to the bolt. The penalty of course is that the member faces lose contact, which could be important in relation to sealing requirements.

Even more extreme non-linear effects on member stiffness were reported previously for a single bolted joint geometry by Grosse and Mitchell [16] in a configuration where the radial bending stiffness of the member was probably much less than in the present example. Lehnhoff *et al* [14] recognised the findings of reference [16] and carried out a parametric survey of different geometries and materials. However, their results misinterpret the significance of non-linearity as their quoted stiffness values are referred to the initial unloaded state rather than to the pre-loaded starting point, which is more relevant to any cyclic loading experienced by the bolts in service. The results of a parametric survey carried out by the present authors show that several variables are significant in the external loading phase, in relation to non-linear behaviour, enhanced member stiffness and loss of contact. These include bolt size, total grip length and the radial position of the external load application. Publication of these results in a form which will facilitate design decisions is planned. However, for the time being, it is clear that the pre-load analysis gives very little insight into the service external loading situation and there is therefore every reason for designers of

bolted joints to optimise proposed designs through specific finite element determinations, especially in situations where a high-performance joint is required.

8.0 Conclusions

- Reasonable agreement between the results of the finite element study and the experimental analysis has been demonstrated.
- Finite element models of bolted joints that do not include the threads and use simplified representations of the bolt head and nut geometry produced results that conformed well to the experimental data. Such an approach is conservative with respect to prediction of the proportion of external load transmitted to the bolt.
- Classical theory of bolted joints has been shown to greatly over-predict the portion of the external load carried by the bolt and is therefore pessimistic in relation to prediction of fatigue strength.

9.0 Acknowledgements

The authors would like to thank Mark Symington, Kenneth Chan and Grahame Guthrie (University of Strathclyde) for their help in collecting the data presented in this paper. The authors also acknowledge the use of the ANSYS v9.0 finite element programme which was made available through an educational licence.

10.0 References

1. Shigley, J.E, 1986, Mechanical Engineering Design, 1st Metric Edition, McGraw Hill
2. Shigley, J.E., Mischke, C.R., 2001, Mechanical Engineering Design, 6th Edition, McGraw Hill
3. Bickford J.H., 1998, *The Handbook of Bolts and Bolted Joints*, Hardback Edition, Dekker
4. Bickford J.H., 1995, *An Introduction to the Design and Behaviour of Bolted Joints*, 3rd Edition, Dekker
5. Norton, R.L., 2000, Machine Design: An Integrated approach, 2nd Edition, Prentice Hall
6. BS EN1591-1:2001, *Flanges and their joints. Design rules for gasketed circular flange connections. Calculation methods.* BSI, London.
7. Abid, M., Nash, D.H., 2004 Comparative study of the behaviour of conventional gasketed and compact non-gasketed flanged pipe joints under bolt up and operating conditions, Int J Pressure Vessels and Piping, 80, 12, 831-841.
8. Pedersen, N.L., Pedersen, P., 2008, *Stiffness Analysis and Improvement of Bolt-Plate Contact Assemblies,* Mechanics Based Design of Structures and Machines, 36: 47-66.
9. Motosh, N, 1976, *Determination of Joint Stiffness in Bolted Connections*, ASME Journal of Industrial Design, 98(3), pp858-861
10. Burguete, R.L., 1992, *Methods to calculate joint stiffness. A review and classification of joint type*s, ASME, *Materials Engineering*, pp 347-354

11. Osgood, C.C., 1979, *Saving Weight on Bolted Joints*, Machine Design, October
12. Wileman, J., Choudhury, M., Green, I., 1991, Computation of Member Stiffness in Bolted Connections, ASME, Journal of Mechanical Design, 113, pp 432-437
13. Lehnhoff, T.F., McKay, M.L., Bellora, V.A., 1992, *Member Stiffness and Bolt Spacing of Bolted Joints*, ASME, Journal of Pressure Vessels and Piping, 248, pp 63-72
14. Lehnhoff, T.F., McKay, M.L., Kwang, K., 1994, *Member Stiffness and Contact Pressure Distribution of Bolted Joints*, ASME, Journal of Mechanical Design, 116, pp 550-557
15. Pedersen, N.L. and Pedersen, P., 2008, *On prestress stiffness analysis of bolt-plate contact assemblies,* Arch Appl Mech, 78: 75-88.
16. Grosse, I.R. and Mitchell, L.D. *Non-linear axial stiffness characteristics of axisymmetric bolted joints,* J of Mechanical Design, Trans ASME, 112,442-449, 1990.
17. ANSYS v9.0, Ansys Inc, Houston, PA.
18. Ito, Y, Toyoda J., Nagada, S. 1977, *Interface Pressure Distribution in a Bolt Flange Assembly*, ASME Paper No. 77-WA/DE-11

Figure Captions

Figure 1: Simple single-bolted joint in tension
Figure 2: Pressure cone envelope
Figure 3: Wire frame representation of test rig
Figure 4: 2D axisymmetric representation of test specimen (dimensions in mm)
Figure 5: 2D axisymmetric finite element model of experiment
Figure 6: Comparison of experimental and FE results – 6 kN pre-load
Figure 7: Comparison of experimental and FE results – 16/17 kN pre-load
Figure 8: Comparison of results with classical theory – 16/17 kN pre-load
Figure 9 (a): axial stress during pre-loading - 8.5 kN pre-load - Advanced Model
Figure 9 (b): axial stress during pre-loading – 17 kN pre-load – Advanced Model
Figure 10 (a): axial stress on application of external load - 8.5 kN external load - Advanced Model
Figure 10 (b): axial stress on application of external load - 17 kN external load - Advanced Model

	υ	E (GPa)	0.2% proof (MPa)
AS 21523 Bi-Hex (Steel) Bolt	0.30	201	590
Rig: Steel (hardened& tempered)	0.30	205	880

Table 1: Material Properties

	μ_s	μ_k
Steel on Steel (dry)	0.8	0.42

Table 2: Coefficients of static and kinematic friction for dry contact

	Test 1	Test 2
Pre-load, F_i	6kN	17kN
External Load, P	5kN	14kN

Table 3: Load Data

		6 kN pre-load		16/17 kN pre-load	
		bolt stiffness	member stiffness	bolt stiffness	member stiffness
Simple model	**Pre-load stage**	0.18E6	0.90E6	0.18E6	0.89E6
	External load stage	0.16E6	4.80E6	0.16E6	4.96E6
Advanced model	**Pre-load stage**	0.18E6	1.06E6	0.18E6	1.11E6
	External load stage	0.17E6	≅ 7.30E6	0.14E6	≅11.1E6

Table 4: Component stiffnesses (N/mm) determined from FE analysis

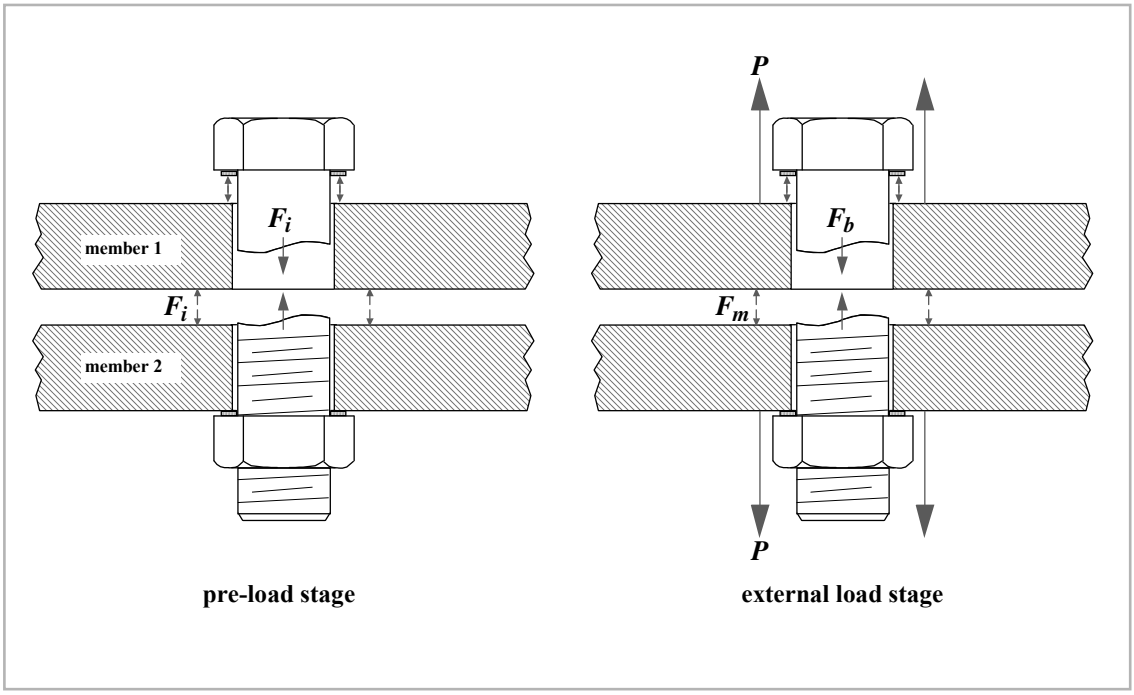

Figure 1: Simple single-bolted joint in tension

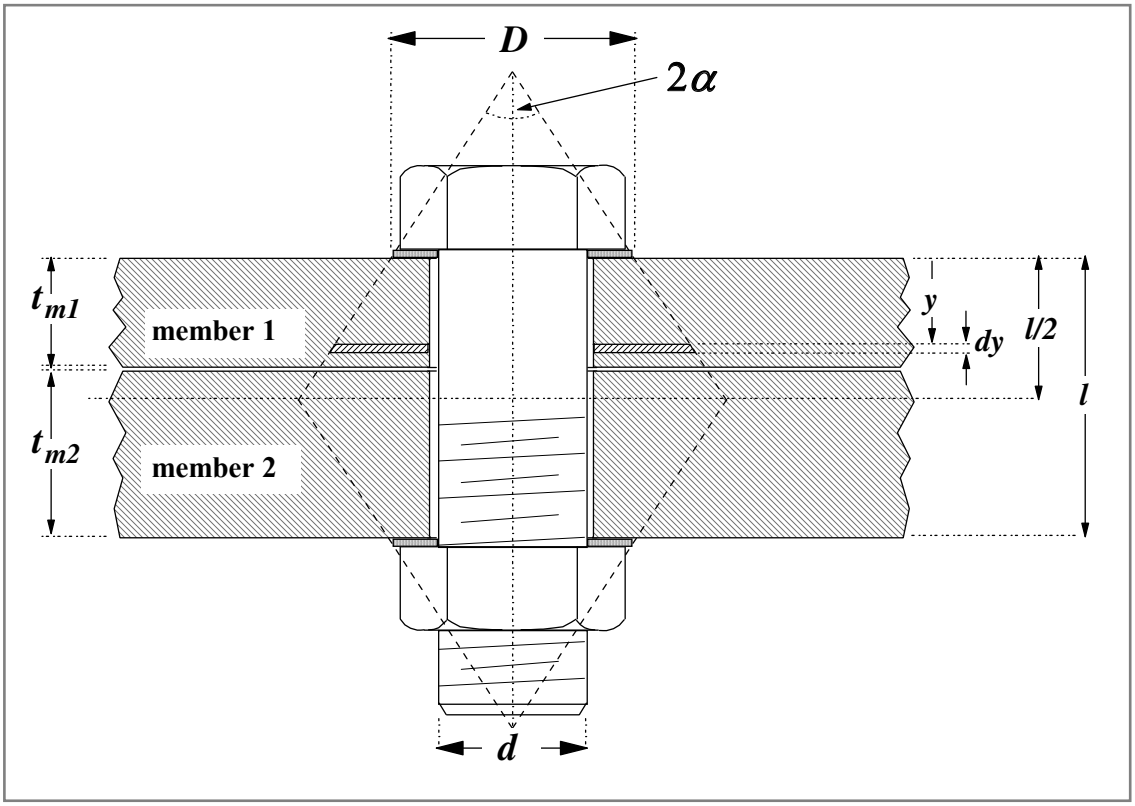

Figure 2: Pressure cone envelope

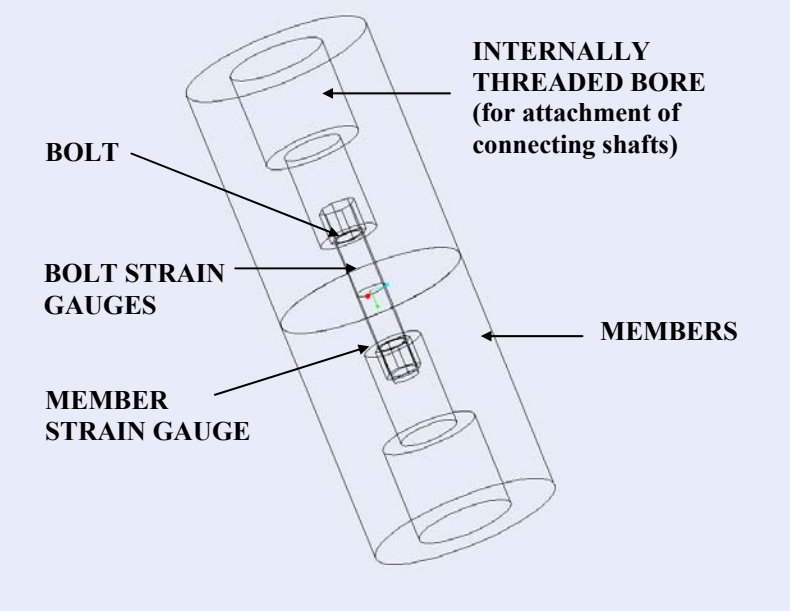

Figure 3: Wire frame representation of test rig

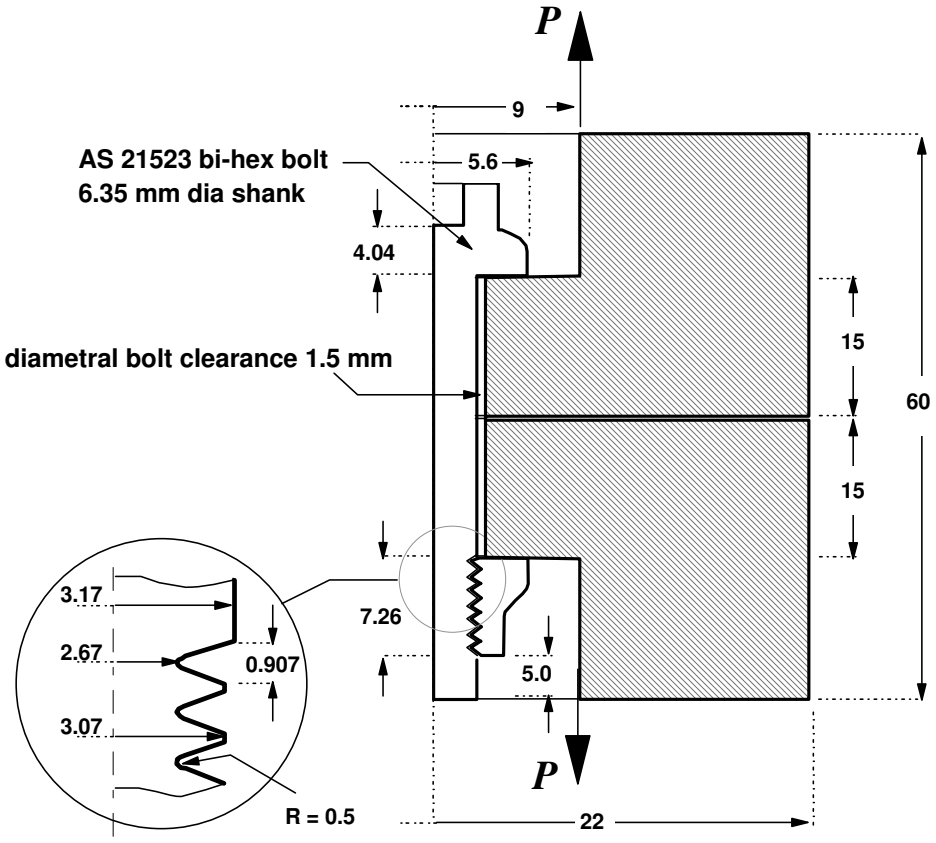

Figure 4: 2D axisymmetric representation of test specimen (dimensions in mm)

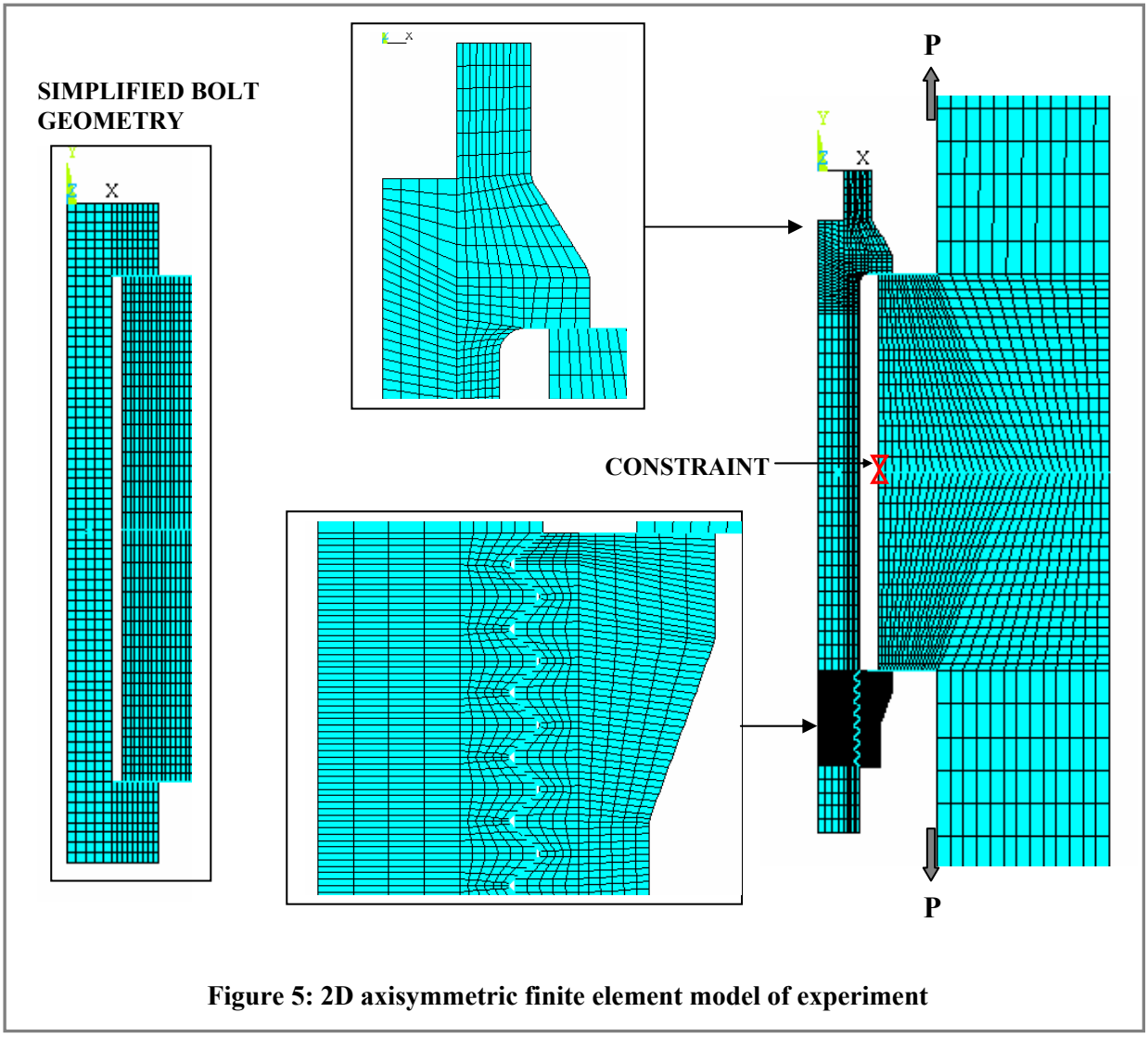

Figure 5: 2D axisymmetric finite element model of experiment

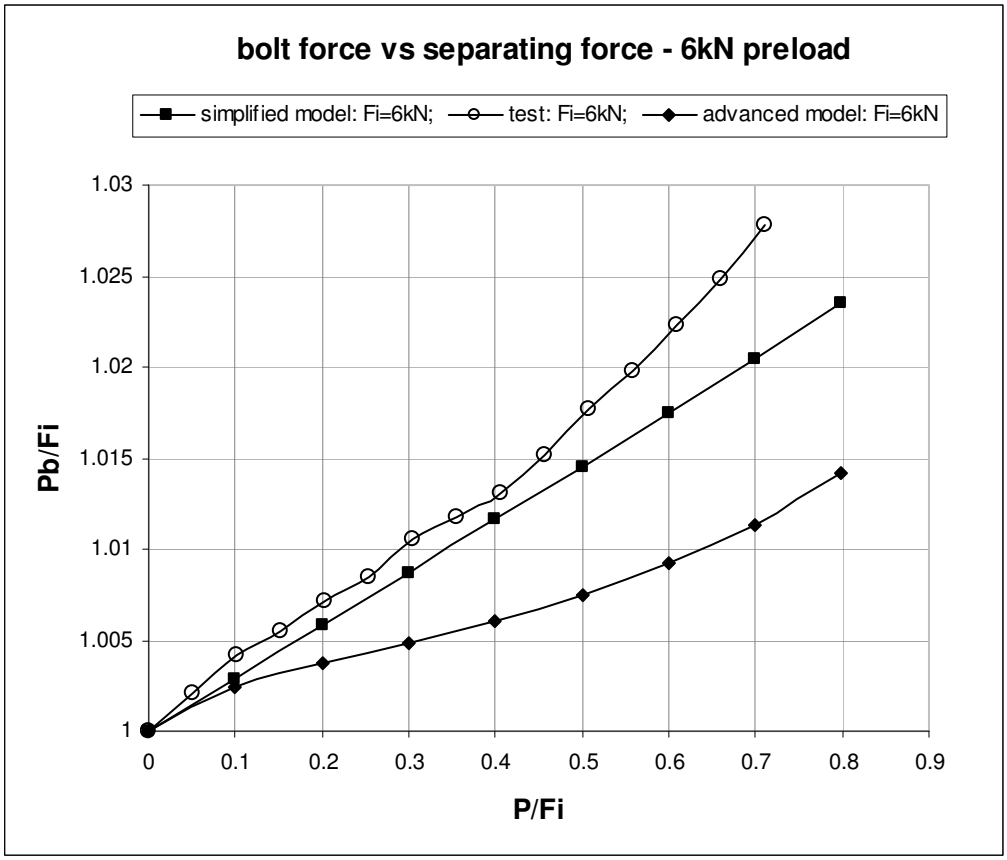

Figure 6: Comparison of experimental and FE results – 6 kN pre-load

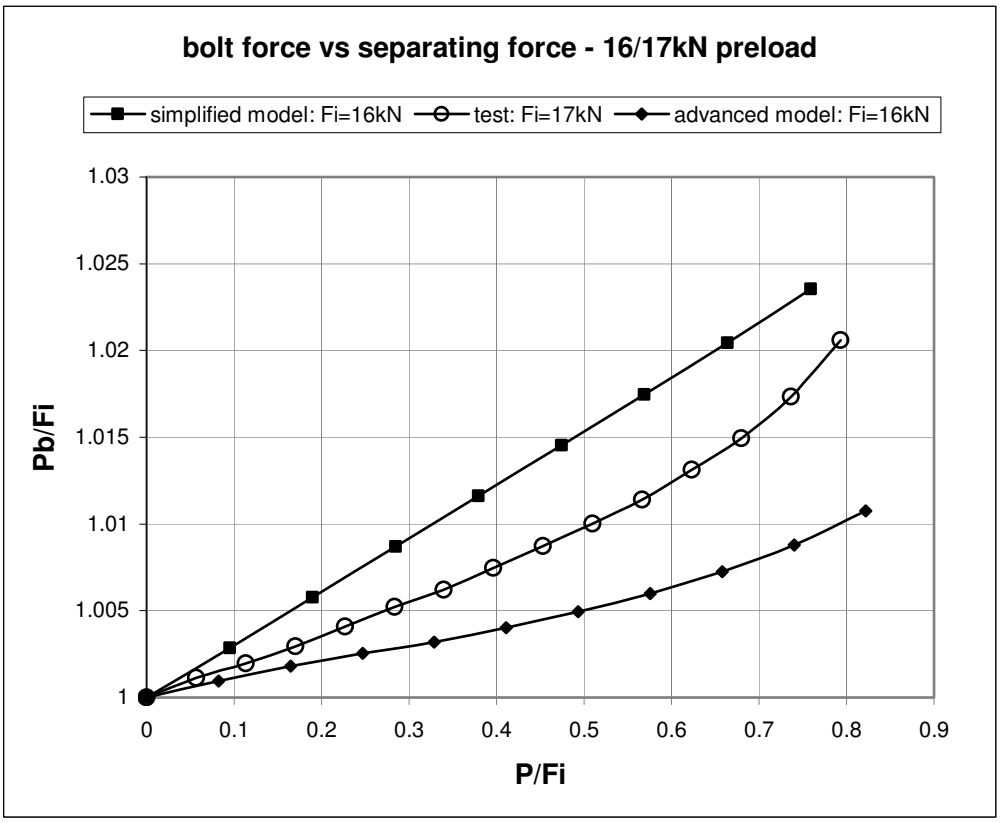

Figure 7: Comparison of experimental and FE results – 16/17 kN pre-load

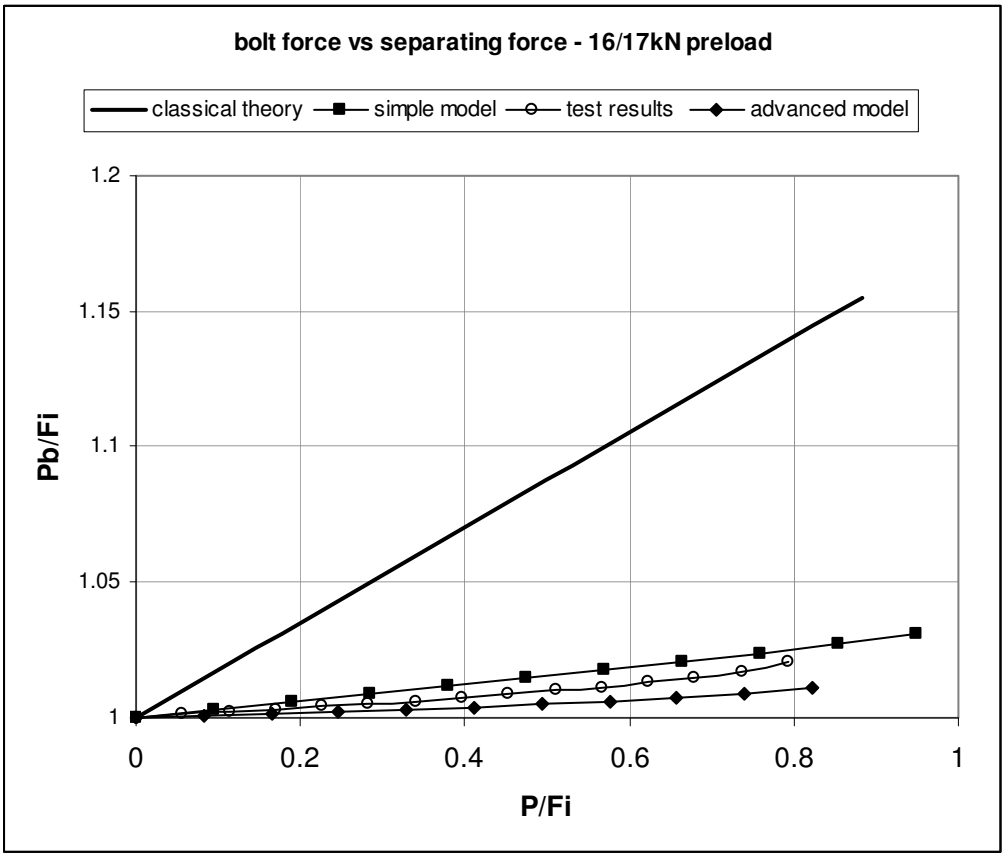

Figure 8: Comparison of results with classical theory – 16/17 kN pre-load

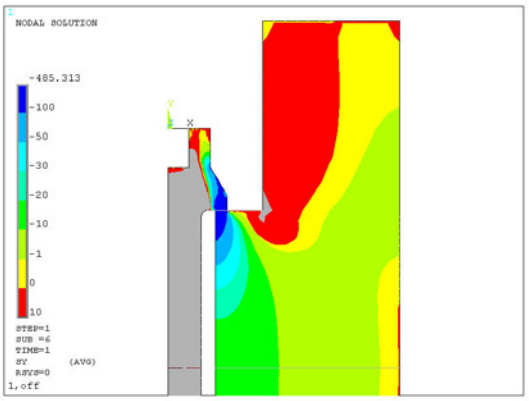

(a) 8.5 kN pre-load - Advanced Model

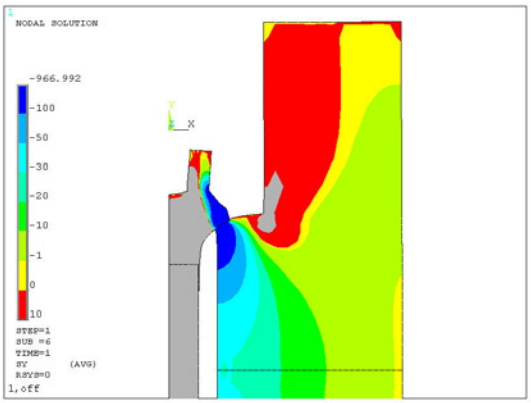

(b) 17 kN pre-load - Advanced Model

Figure 9: axial stress during pre-loading

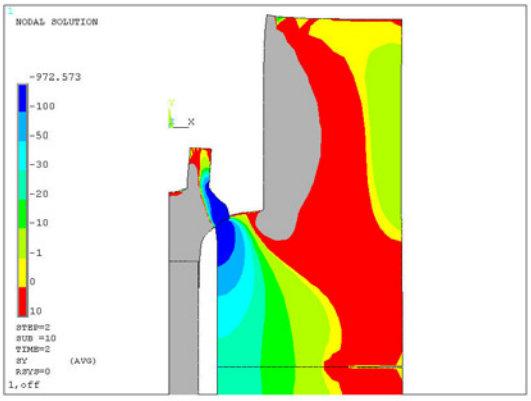

(a) 8.5 kN external load - Advanced Model

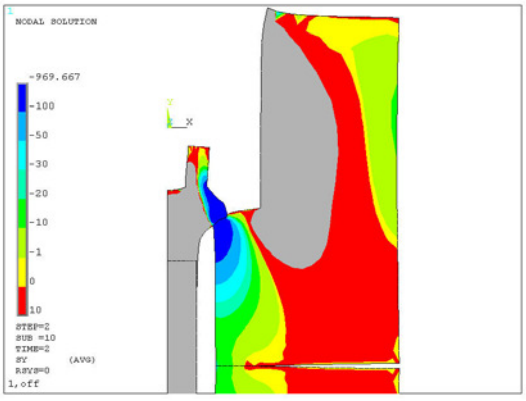

(b) 17 kN external load - Advanced Model

Figure 10: axial stress on application of external load